Electrochimica Acta 283 (2018) 1203–1212

Contents lists available at ScienceDirect

Electrochimica Acta

journal homepage: www.elsevier.com/locate/electacta

Enhanced electrochemical performance of perovskite $LaNiO_3$ coating on $Li_{1.2}Mn_{0.54}Ni_{0.13}Co_{0.13}O_2$ as cathode materials for Li-ion batteries

Xiaodong Zhang [a], Junjie Hao [a,*], Licheng Wu [a], Zhimeng Guo [a], Zhenhui Ji [a], Ji Luo [a], Cunguang Chen [a], Jinfeng Shu [a], Haiming Long [a], Fang Yang [a], Alex A. Volinsky [b]

[a] Institute for Advanced Materials and Technology, University of Science and Technology Beijing, 30 Xueyuan Road, Haidian District, Beijing, 100083, China
[b] Department of Mechanical Engineering, University of South Florida, Tampa, FL 33620, USA

ARTICLE INFO

Article history:
Received 4 January 2018
Received in revised form
22 May 2018
Accepted 11 July 2018
Available online 17 July 2018

Keywords:
Lanthanum nickel oxide
Coating
Lithium-rich
Layered oxides
Cathode

ABSTRACT

$LaNiO_3$ thin film coated Li-rich cathode $Li_{1.2}Mn_{0.54}Ni_{0.13}Co_{0.13}O_2$ material is fabricated for the first time using the facile sol-gel process. Morphology, structure and battery cycle performance of the $LaNiO_3$-coated $Li_{1.2}Mn_{0.54}Ni_{0.13}Co_{0.13}O_2$ is characterized by a series of tests. $LaNiO_3$ coating was synthesized by the sol-gel process and uniformly covered powder surface. By coating proper amount of $LaNiO_3$, the initial Coulombic efficiency, discharge capacity, rate capability and cycle performance are significantly improved, while the charge transfer resistance reduces. The initial Coulombic efficiency of 3 wt% $LaNiO_3$-coating samples reaches the maximum of 70% and 65% at 0.1 C and 1 C rates, respectively. The 3 wt% $LaNiO_3$-coating electrode has the highest initial charge/discharge capacity of 405.4/285.1 mAh g^{-1} at 0.1 C rate (1 C = 250 mA g^{-1}), while 5 wt% $LaNiO_3$-coating delivers the maximum value of 264.1/165.1 mAh g^{-1} at 1 C. The cycling performance profiles demonstrate that at 1 C rate, the 3 wt% $LaNiO_3$-coated electrode exhibits higher discharge specific capacity of 207.6 mAh g^{-1} and cyclic stability of 190.3 mAh g^{-1} 92% capacity retention after 50 cycles compared with pristine and other content $LaNiO_3$. The film resistance and charge transfer resistance both decrease after coating with $LaNiO_3$. $LaNiO_3$ is an efficient modifier to enhance electrochemical performance of Li-rich cathode materials.

1. Introduction

More and more lithium-ion batteries (LIBs) are used in electrical devices, especially in hybrid electric vehicles (HEV) and electric vehicles (EV) [1,2]. However, conventional cathode materials, such as layered $LiCoO_2$ [3], spinel $LiMnO_4$ [4] and olivine $LiFeO_4$ [5] cannot meet the requirements of high energy density due to limited specific capacity.

In recent years, Li-rich layered cathode materials, $Li_{1.2}Mn_{0.54}Ni_{0.13}Co_{0.13}O_2$ (LMNC), have drawn considerable attention due to certain advantages, such as high discharge capacity (>250 mAh g^{-1}), high operation voltage (4.6–4.8 V Li/Li^+), lower cost, low toxicity and high safety, which shows great potential for applications in EVs and HEVs [6–9]. LMNCs consist of solid solution of Li_2MnO_3 and $LiMO_2$ (M = Ni, Co, Mn or their combination).

Due to large irreversible capacity loss [10–12], poor rate capacity [7,12,13], severe cyclic capacity fading [10,14,15], Li-rich cathode materials are not commercially available. Enormous research efforts have been undertaken to eliminate disadvantages of Li-rich cathodes, including structure and morphology optimization [16,17], mild acidic treatment [18–20], cationic substitution [20–23] and composite cathodes.

Among these approaches, surface coatings modification has been proved as an effective method to solve the problems of low cycling stability and poor rate capability. Various surface coatings, including carbon, metal oxides (Al_2O_3, CaO, TiO_2, La_2O_3, MgO, ZrO_2, ZnO, MnO_2), metal fluorides (AlF_3, CeF_3), and metal phosphates ($AlPO_4$, $FePO_4$) have been applied to generate a barrier between electrolyte and electrode, enhancing electrochemical properties and prolonging life cycle [24–29]. Nevertheless, some of the coatings lead to variations in electrical conductivity and reduced capacity due to week activity and high resistance.

Perovskite (ABO_3) type complex oxides, such as lithium lanthanum titanate (LLTO) $Li_{3x}La_{(2/3)-x}\square_{(1/3)-2x}TiO_3$, are the best crystalline inorganic Li ion-conducting solid electrolyte materials. LLTO shows high Li ion conduction up to 10^{-3} S/cm

* Corresponding author.
E-mail address: haojunjie@ustb.edu.cn (J. Hao).

https://doi.org/10.1016/j.electacta.2018.07.057
0013-4686/

($E_a = 0.3–0.4$ eV) at room temperature for $x = 0.11$ [30].

Lanthanum nickel oxide $LaNiO_3$ (LNO) with pseudo-cubic perovskite structure ($a = 3.84$ Å) is widely used in many applications, including dielectric material electrodes, solid electrolytes [31–33], sensors and solid resistors. Compared with metal oxides surface coating, $LaNiO_3$ has higher Li ion conduction, high activity and lower resistivity (225 μΩ cm) [34,35]. At the same time, $LaNiO_3$ has better thermal and chemical stability. $LaNiO_3$ (R-3c space group) and LMNC (R-3m space group) have the Ni–O bonds, which promote even stronger combination between them. Due to all these advantages, $LaNiO_3$ is a promising coating material to effectively modify LMNC to enhance rate capability and cycling performance. However, as far as we know, surface coatings modification with $LaNiO_3$ has not been reported yet to treat Li-rich layered cathode materials.

In present experiment, $LaNiO_3$ thin film coated Li-rich cathode material, $Li_{1.2}Mn_{0.54}Ni_{0.13}Co_{0.13}O_2$, was prepared successfully via the sol-gel method for the first time. The structure and morphology are discussed in detail. Various experiments and characterization indicated that the $LaNiO_3$ surface coating can obviously improve the rate capability and the cyclic performance of LMNC cathode material used for LIBs.

2. Experimental details

2.1. Samples preparation

First, homogeneous and transparent solution was mixed by dissolving 1 mol MSO_4 in 0.5 L deionized water. MSO_4 consisted of $NiSO_4$, $CoSO_4$, $MnSO_4$ in cationic ratio of Ni:Co:Mn = 0.13:0.13:0.54. The solution with a concentration of 1 $molL^{-1}$ was injected into 1 L volumetric flasks and deionized water was added to raise the liquid level to the 1 L gradation line. At the same time, 1 $molL^{-1}$ $NaCO_3$ solution was adjusted to pH of 8 using ammonia, which was also added as chelating agent. Two solutions were carefully dropped into a continuous stirring reactor at 60 °C. After washing by alcohol, vacuum filtration and vacuum drying, the co-precipitation carbonate precursor $(Mn_{0.54}Ni_{0.13}Co_{0.13})CO_3$ was milled (5% mole ratio) with an excess amount of lithium carbonate for 6 h by the planetary mill in alcohol. After alcohol completely evaporated, the mixture was calcined at 550 °C for 5 h and 850 °C for 10 h with a heating rate of 5 °C/min in air. Thus, pristine layered $Li_{1.2}Mn_{0.54}Ni_{0.13}Co_{0.13}O_2$ powder was finally obtained by carbonate co-precipitation through the above steps.

The second step was to prepare the $LaNiO_3$-coating on the $Li_{1.2}Mn_{0.54}Ni_{0.13}Co_{0.13}O_2$ cathode material. The same molar ratio of $La(NO_3)_3 \cdot 6H_2O$ and $Ni(NO_3)_2 \cdot 6H_2O$ was blended with a proper amount of citric acid and ethylene glycol accompanied by constant stirring to obtain green solution. The solution was mixed with $Li_{1.2}Mn_{0.54}Ni_{0.13}Co_{0.13}O_2$ at 80 °C and stirred until the formation of stable black sol. The sol was placed into 100 °C incubator to prepare gel. In the end, black powder was obtained by heating the gel to 850 °C for 30 min, which was $Li_{1.2}Mn_{0.54}Ni_{0.13}Co_{0.13}O_2$ coated with $LaNiO_3$.

2.2. Characterization

The phase composition and distribution of elements of the powders were analyzed by X-ray diffraction analysis (XRD, TTRIII) and electron diffraction spectroscopy (EDS), respectively. The microstructure and morphology of the particles were observed by a field emission scanning electron microscope (FESEM, LEO 1450) and high-resolution transmission electron microscopy (HRSTEM Tecnai G2 F30 S-TWIN).

2.3. Electrochemical measurements

$LaNiO_3$-coated $Li_{1.2}Mn_{0.54}Ni_{0.13}Co_{0.13}O_2$ as cathode active substance, acetylene black as conductive agents and polyvinylidene fluoride (PVDF) as binder (at a mass ratio of 8:1:1) were dispersed to N-methyl-2-pyrrolidone (NMP) solvent preparing black slurry with good flow properties. The slurry was coated on clean aluminum foil by blade tape casting with 0.04 mm gap. The tapes were cut into a wafer with 1.4 cm diameter after drying at 120 °C for 12 h.

The CR2032 type coin cells were assembled in Ar-filled glove box. The coin cells consisted of cathode, separator, electrolyte and counter electrode, which was made of as-prepared $LaNiO_3$-coated $Li_{1.2}Mn_{0.54}Ni_{0.13}Co_{0.13}O_2$, Cellgard 2400 polypropylene film, 1 $molL^{-1}$ $LiPF_6$ dissolved in ethylene carbonate (EC)/ethyl methyl carbonate (EMC)/dimethyl carbonate(DEC) (1:1:1 ratio by volume) and lithium metal, respectively. The DC charge discharge tests were performed using a battery test system (Land CT2001A, Wuhan Jinnuo Electronic Co. Ltd) between 2 V and 4.8 V (vs. Li^+/Li) at room temperature. Electrochemical impedance spectroscopy (EIS) experiments were carried out to investigate the impedance change of the samples prepared with pristine and $LaNiO_3$-coated LMNC using the CHI600E electrochemical workstation.

3. Results and discussion

3.1. Materials characterization

Fig. 1 shows XRD patterns of pristine powder and $LaNiO_3$-coated samples of $Li_{1.2}Mn_{0.54}Ni_{0.13}Co_{0.13}O_2$. Most of the diffraction reflections can be indexed to the α-Na-FeO_2 structure based on the trigonal R-3m structure [36], except for the weak peaks between 20° and 25°, which are indexed based on the monoclinic ($C2/m$) structure (super lattice of Li_2MnO_3) [36–38].

The peaks intensity of $LaNiO_3$ was increasing with $LaNiO_3$ (x, mass percentage) additive content, while the intensity of the XRD pattern peaks decreased for the top two peaks (003) and (104), shown in Table 1. The XRD pattern indicates that $LaNiO_3$ and $Li_{1.2}Mn_{0.54}Ni_{0.13}Co_{0.13}O_2$ powder reacted and successfully formed a compound, which could not be washed. It is believed that the $LaNiO_3$ coating has little effect on the host structure of LMNC particles, especially when $x = 1\%$ and 2%. When the $LaNiO_3$ content was increased to 5%, secondary $LaNiO_3$ phase could be clearly identified.

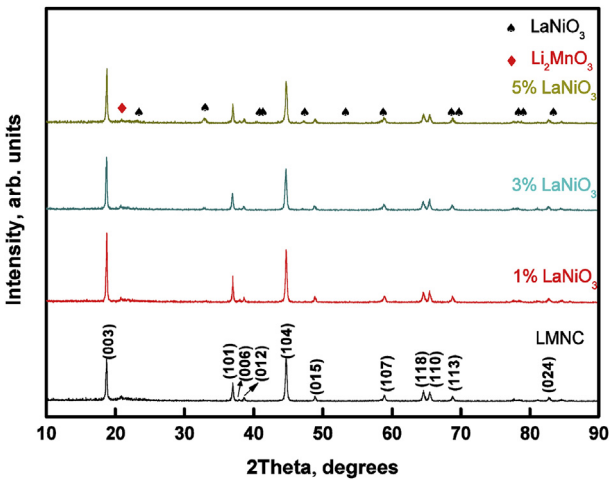

Fig. 1. XRD patterns of pristine and $LaNiO_3$-coated LMNC with different $LaNiO_3$ content.

Table 1
Structure parameters for $Li_{1.2}Ni_{0.13}Co_{0.13}Mn_{0.54}O_2$ from XRD patterns.

$LaNiO_3$ wt.%	$I_{(003)}$	$I_{(104)}$	$I_{(003)}/I_{(104)}$	a, Å	c, Å	c/a	Volume Å^3	$R=(I_{(102)}+I_{(006)})/I_{(101)}$
0	441	318	1.39	2.848	14.22	4.993	99.88	0.343
1	399	291	1.37	2.849	14.226	4.993	100.11	0.301
3	366	280	1.31	2.847	14.2	4.988	99.68	0.306
5	351	270	1.3	2.846	14.215	4.995	99.71	0.312

The splitting of the (006)/(102) and (108)/(110) peaks was observed in all samples. This indicates that the treated samples still have highly ordered layered hexagonal structure [13,39].

As shown in Table 1, the lattice parameter (a, c), the trigonal distortion (c/a) and the cell volume have no obvious changes, in good agreement with the literature [40–42]. The intensity ratio of (003) and (104) planes ($I_{(003)}/I_{(104)}$), which was calculated as 1.3–1.39 (>1.2) response, corresponding to different content of $LaNiO_3$. The R-factor ($(I_{(102)}+I_{(006)})/I_{(101)}$) for all samples is calculated to be in the 0.301–0.343 range. Both I(003)/I(104) and the R-factor confirm that the active substance material has a layered structure with hexagonal ordering (O^3 type) [36,37,39–42].

3.2. Morphology and structure of pristine and $LaNiO_3$-coated $Li_{1.2}Mn_{0.54}Ni_{0.13}Co_{0.13}O_2$

SEM characterization was carried out to observe the surface morphology of $Li_{1.2}Mn_{0.54}Ni_{0.13}Co_{0.13}O_2$ and $LaNiO_3$-coated $Li_{1.2}Mn_{0.54}Ni_{0.13}Co_{0.13}O_2$ samples. As shown in Fig. 2, the pristine LMNC powders are nearly spherical or oval with an average diameter of 10 μm and rough surface morphology. Higher magnification shows that the spherical particles are composed of a great amount of primary particles with 200–300 nm size and smooth surface. This morphology is beneficial for improving the filling capacity of active material and the contact area to the electrolyte, which greatly affects the cell performance. There was no obvious difference in morphology between LMNC and $LaNiO_3$-coated LMNC samples for the relatively low coating amount of $LaNiO_3$. It is believable that the $LaNiO_3$ layer is thin on the $Li_{1.2}Mn_{0.54}Ni_{0.13}Co_{0.13}O_2$ surface, which was further confirmed by TEM.

EDS was conducted to identify elements of $LaNiO_3$ coating layer on the surface of 3 wt% $LaNiO_3$-coated $Li_{1.2}Mn_{0.54}Ni_{0.13}Co_{0.13}O_2$, as shown in Fig. 3. For each material, the result of only one of the three treated powders is shown, since the differences within each kind are rather small (see Fig. 2). Fig. 3(a), and (b) present the cross-section of several hollow spherical particles after agglomeration by primary particles. It also proves that the near-spherical $Li_{1.2}Mn_{0.54}Ni_{0.13}Co_{0.13}O_2$ particle has a core-shell structure with the 1.5–3 μm wall thickness. As shown in Fig. 3(a) and (b), the brighter places were proven to be a series of $LaNiO_3$ accumulation areas on the particle surface because La has larger atomic number, which presents higher brightness in electron back scattered diffraction (EBSD) image. In Fig. 3(c) and (d), the amount of Mn, Ni, Co decreases along the outward radial direction of particle diameter, and the La content increases where there is no brighter La accumulation area. In addition, Fig. 3(e) shows elements identification of Mn, Ni, Co and La in the red frame region in Fig. 3(b). Thus, the $LaNiO_3$ layer is evenly distributed on the surface of agglomeration particles.

Fig. 4 shows surface morphology and microstructure of pristine and $LaNiO_3$-coated $Li_{1.2}Ni_{0.13}Co_{0.13}Mn_{0.54}O_2$ particle observed by HR-TEM. The primary particles have smooth surface and edge, as seen in Fig. 4(a, d). Comparing Fig. 4(b) and (e), we have proven the homogeneity of $LaNiO_3$-coating surrounding the primary particles. A thin film with 2–3 μm thickness has formed on the surface of the particle in Fig. 4(e). That is why there is no obvious difference in particle size and morphology of the surface modification with $LaNiO_3$. Fig. 4(f) shows $LaNiO_3$ accumulation area on the $Li_{1.2}Ni_{0.13}Co_{0.13}Mn_{0.54}O_2$ particle with non-uniform thickness, which was coincident with the brighter spot in the EDS image. In

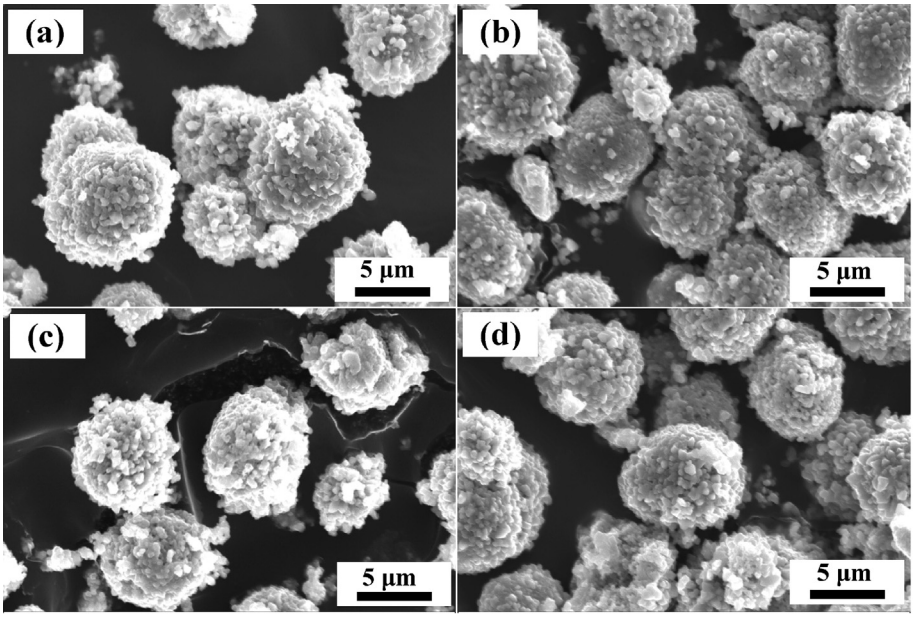

Fig. 2. SEM images of LMNC treated with LaNiO3: (a) pristine, (b) 1%, (c) 3%, (d) 5%.

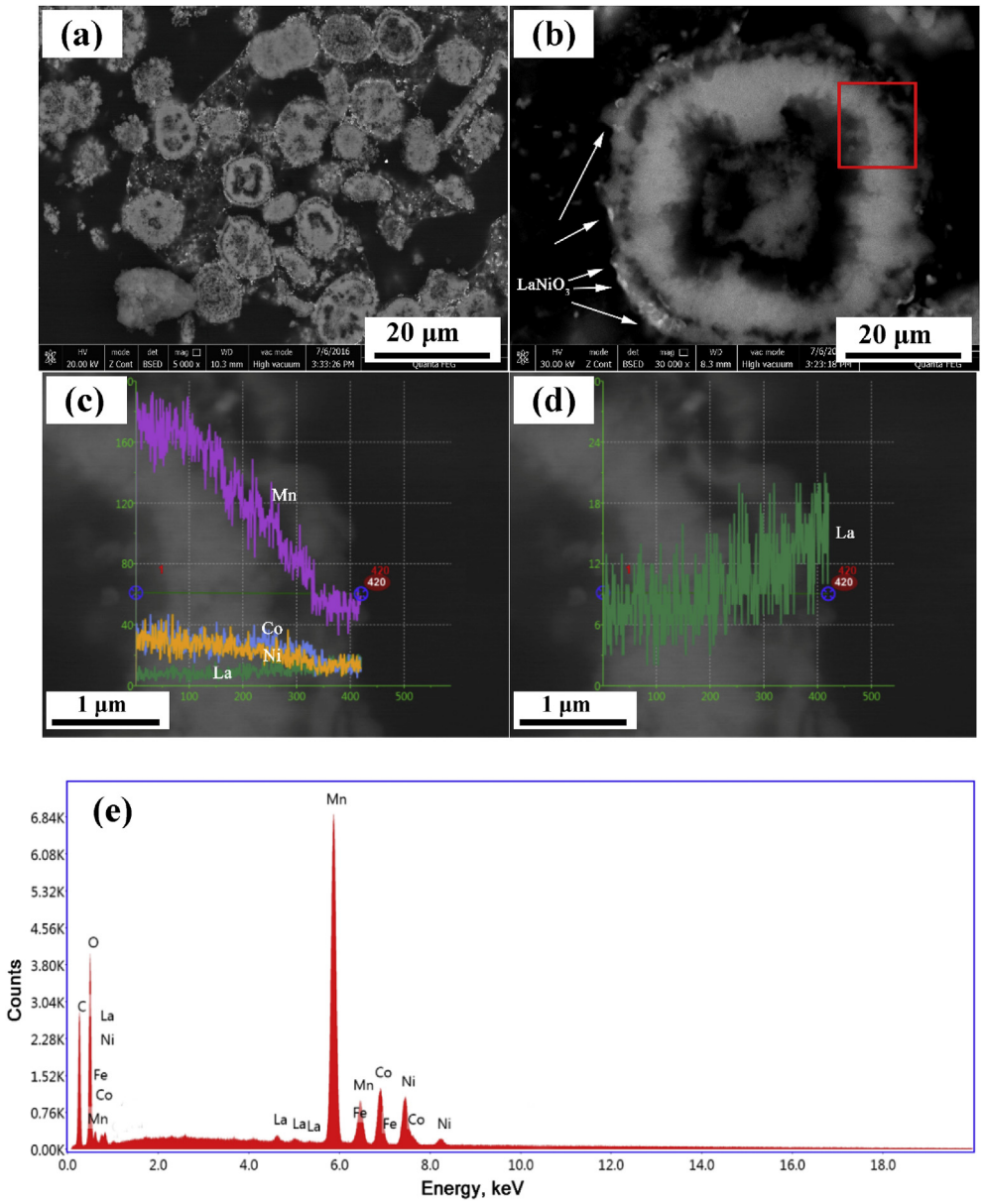

Fig. 3. FESEM images and EDS of the 3 wt% LaNiO3-coated LMNC particle cross-section: (a) and (b) BSED, (c) and (d) EDS line scans of elements, (e) EDS of elements identification.

addition, it also confirmed good adhesion between the $LaNiO_3$-coating layer and the core material where there is no clear interface.

It is clearly noted that the crystal plane spacing of 0.477 nm corresponds to the (003) crystal plane of the layered R3-m phase of $Li_{1.2}Ni_{0.13}Co_{0.13}Mn_{0.54}O_2$ from the HR-TEM images and the fast Fourier transform pattern images in Fig. 4(c, f). There is no obvious change in structure of the $Li_{1.2}Ni_{0.13}Co_{0.13}Mn_{0.54}O_2$ phase after coating. The HR-TEM revealed the formation of the coating layer, which agrees with the above XRD results. The $LaNiO_3$ coating layers can protect active materials from direct contact with the electrolyte and thus can suppress the occurrence of side reactions. In addition, the $LaNiO_3$ layer would facilitate the transport of Li ions across the surface compared to other coating layers.

3.3. Electrochemical performance

The electrochemical properties of the samples were measured by using assembled coin-type cells. Fig. 5 shows the first charge-discharge profile of the pristine and $LaNiO_3$-coated $Li_{1.2}Mn_{0.54}Ni_{0.13}Co_{0.13}O_2$ electrodes at a constant current density of 0.1 C and 1 C (1 C = 250 mA g^{-1}) between 2 V and 4.8 V. As seen from Fig. 5, the initial charge/discharge profiles are in agreement with other reported Li-enriched cathodes [27,38,43]. Similarly, all the samples exhibit two plateau regions in the first charge profile when voltage is about 4 V and 4.5 V, respectively. According to XRD results, the precipitate of $Li_{1.2}Mn_{0.54}Ni_{0.13}Co_{0.13}O_2$ was recognized to be a mixture of the trigonal R-3m structure and the monoclinic ($C2/m$) structure, which can be written as $xLi_2MnO_3 \cdot (1.2\text{-}2x)\ LiMO_2$ (M = Co, Ni or Mn). It is generally accepted that $Li_{1.2}Mn_{0.54}Ni_{0.13}Co_{0.13}O_2$ electrodes are charged by two steps with different mechanisms during the first charging process. This behavior can be explained as follows.

Charging

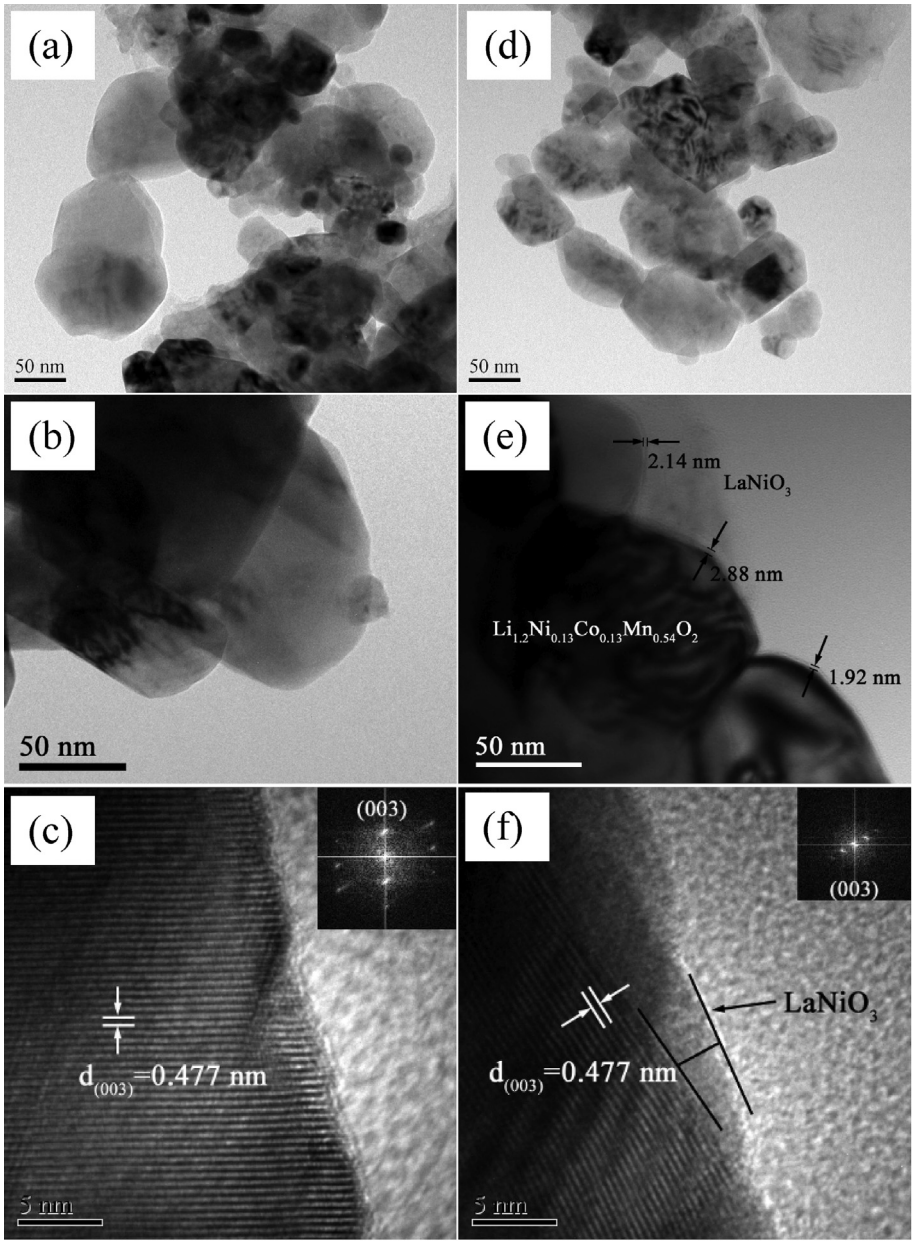

Fig. 4. HRTEM images of pristine (a, b, c) and LaNiO3-coated (d, e, f) LMNC particle with the fast Fourier transform pattern (FFT).

$$x\mathrm{Li_2MnO_3}\cdot(1.2\text{-}2x)\mathrm{LiMO_2} \rightarrow x\mathrm{Li_2MnO_3}\cdot(1.2\text{-}2x)\mathrm{MO_2} + (1.2\text{-}2x)\ \mathrm{Li^+} + (1.2\text{-}2x)\mathrm{e^-} \quad (1)$$

$$x\mathrm{Li_2MnO_3}\cdot(1.2\text{-}2x)\mathrm{MO_2} \rightarrow x\mathrm{MnO_2}\cdot(1.2\text{-}2x)\mathrm{MO_2} + 1/2x\ \mathrm{O_2} + 2x\ \mathrm{Li^+} + 2x\ \mathrm{e^-} \quad (2)$$

Discharging

$$x\mathrm{MnO_2}\cdot(1.2\text{-}2x)\mathrm{MO_2} + (1.2\text{-}x)\ \mathrm{Li^+} + (1.2\text{-}x)\mathrm{e^-} \rightarrow x\mathrm{LiMnO_2}\cdot(1.2\text{-}2x)\ \mathrm{LiMO_2} \quad (3)$$

The chemical reaction (1) takes place at about 4 V, which is corresponding to the Li^+ extraction from the structure of space group R-3m, and the oxidation of Ni^{2+} to Ni^{4+} and Co^{3+} to Co^{4+}. It is now generally accepted that the charging reaction (2) in the second sloping section at about 4.5 V is associated with the removal of Li_2O from the Li_2MnO_3-like region accompanied by the generation of oxide ion vacancies. Reaction (2) appears only in the initial cycle, indicating that oxygen loss during first charging is an irreversible process. The large irreversible capacity (CIRR) loss is mainly due to the elimination of the oxide ion vacancies and the lithium ion sites, as well as side reactions with the electrolyte at the high operating voltage over 4.5 V [27,38,43], as shown in Table 2 and Fig. 7. In addition, it can be seen from Fig. 5 that the charge voltage plateau is lowered, while the discharge plateau is elevated by coating with 1–5 wt% $LaNiO_3$. This phenomenon is likely ascribed to improved electronic conductivity and lithium ion transfer promoted by coatings [43,44]. It has to be mentioned that the first discharge capacity increased as the discharge plateau decreased below 3 V regions where the discharge voltage sharply drops.

The first charge/discharge capacity, irreversible capacity and initial Coulomb efficiency values of the pristine and surface-modified samples at 0.1 C and 1 C are given in Table 2. At 0.1 C, the initial charge and discharge capacity of the pristine material is

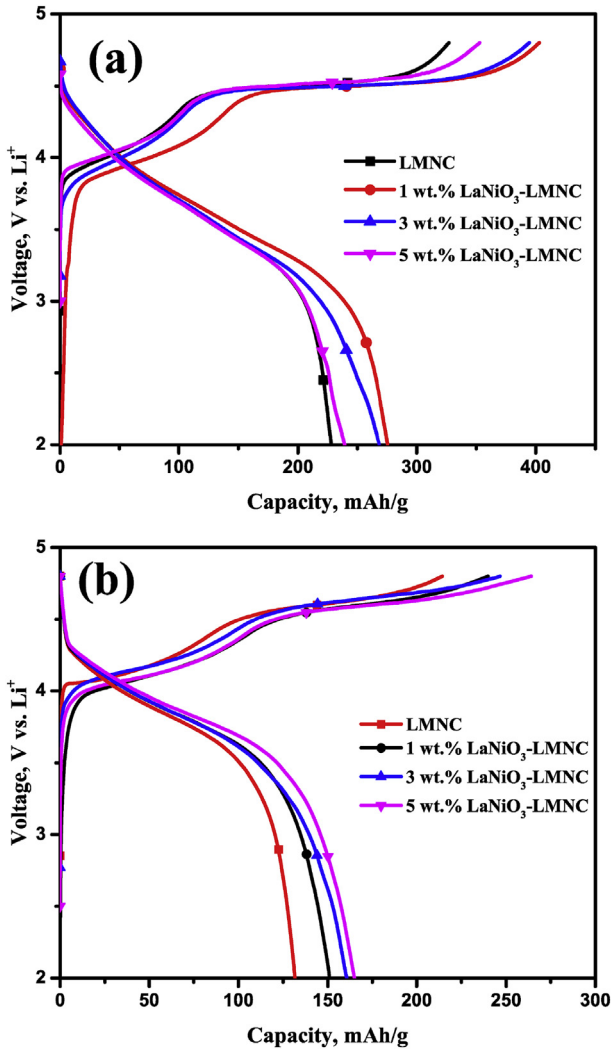

Fig. 5. Initial charge/discharge profiles of LMNC and $LaNiO_3$-coated LMNC electrodes between 2 and 4.8 V at a constant current density: (a) 0.1 C and (b) 1 C.

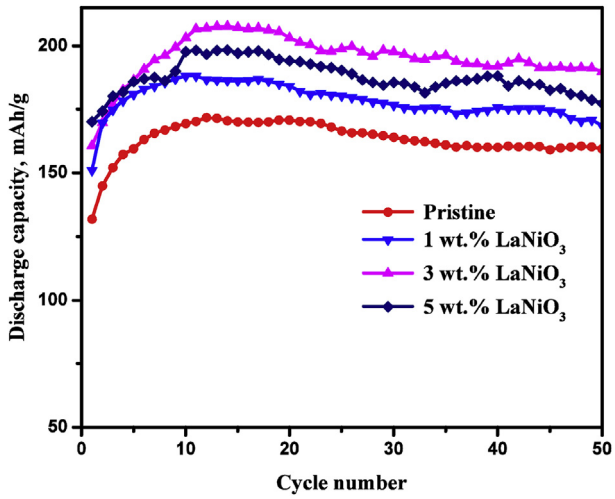

Fig. 6. Cycling performance of LMNC and $LaNiO_3$-coated LMNC electrodes during 50 cycles at 1 C between 2 and 4.8 V.

378 mAh g^{-1} and 246.1 mAh g^{-1}, corresponding to the Coulombic efficiency of 65%. However, for the test at 1 C, the three performance indicators of the pristine material are 214.4 mAh g^{-1}, 131.8 mAh g^{-1} and 61%. In general, compared with the pristine sample, the $LaNiO_3$-coated samples show that the first charge/discharge capacity and the Coulombic efficiency were both elevated at 0.1 C and 1 C. Notably, the initial charge/discharge capacity reaches a maximum of 405.4/285.1 mAh g^{-1} and 264.1/165.1 mAh g^{-1} at 0.1 C and 1 C, coated with 3 wt% and 5 wt% $LaNiO_3$, respectively. The maximum of the initial Coulombic efficiency is 70% and 65% at 0.1 C and 1 C with 3 wt% $LaNiO_3$. As for the increase in the first charge/discharge capacity, it could possibly be attributed to the $LaNiO_3$ coating layer that protects $Li_{1.2}Mn_{0.54}Ni_{0.13}Co_{0.13}O_2$ from the side reactions of the electrolyte, which avoids structural degradation of the layered crystal lattice of the material [45]. However, the increase in $LaNiO_3$ content from 3% to 5% leads to a decrease in the first discharge capacity and the Coulombic efficiency at 0.1 C. This could possibly be ascribed to excessive $LaNiO_3$ coating, which might result in increasing the Li ion conductivity and depressing the electronic transduction, which degrades the capacity of the layered structure. It can be concluded that 3–5 wt% of the electrochemically-active $LaNiO_3$ with pseudo-cubic peroskite structure can effectively increase the initial discharge capacity of LMNC.

Fig. 6 shows the discharge capacity cyclability of cells based on lithium metals as the anode and the $Li_{1.2}Mn_{0.54}Ni_{0.13}Co_{0.13}O_2$ and $LaNiO_3$-coated $Li_{1.2}Mn_{0.54}Ni_{0.13}Co_{0.13}O_2$ as the cathode, tested at 1 C. The discharge capacity results are summarized in Table 3, where a gradual increase in discharge capacity can be identified.

Interestingly, from Fig. 6, the initial discharge capacity of almost all samples is low, then increases and gradually decays during continuous cycling. From Fig. 6 and Table 3, the initial, the maximum and the 50th cycle discharge capacity increases with the $LaNiO_3$ content. When the coating content is higher than 3 wt%, the initial discharge capacity increases with more $LaNiO_3$, while the discharge capacity of later cycles obviously decreases at the same time. Apparently, the 3 wt% $LaNiO_3$-coated $Li_{1.2}Mn_{0.54}Ni_{0.13}Co_{0.13}O_2$ samples exhibit the highest discharge capacity compared to pristine and other content of $LaNiO_3$ during 50 cycles.

Results in Table 3 indicate that the $Li_{1.2}Mn_{0.54}Ni_{0.13}Co_{0.13}O_2$ has the initial discharge capacity of 131.8 mAh g^{-1}, reaching the maximum of 171.7 mAh g^{-1} in the 12th cycle and retaining

Table 2
The first charge/discharge capacity, irreversible capacity and initial Coulombic efficiency values for the pristine and surface-modified samples at 0.1 C and 1C.

$LaNiO_3$ wt.%	Initial Cycle Capacity, mAh g^{-1}							
	0.1 C				1 C			
	Charge	Discharge	Loss	Coulomb efficiency, %	Charge	Discharge	Loss	Coulomb efficiency, %
0	378.0	246.1	131.9	65	214.4	131.8	82.6	61
1	380.4	250.8	129.6	66	239.5	151.0	78.8	63
3	405.4	285.1	120.3	70	246.7	160.7	95.7	65
5	394.6	268.4	126.2	68	264.1	165.1	99	63

Table 3
Discharge capacity values for the pristine and surface-modified samples at 1 C rate.

$LaNiO_3$ wt.%	Discharge Capacity at 1 C			
	Initial cycle mAh g^{-1}	Maximum mAh g^{-1}	50th cycle mAh g^{-1}	Capacity retention %
0	131.8	171.7	159.1	92
1	151	188.2	168	89
3	160.7	207.6	190.3	92
5	165.1	201.7	175.5	87

166.1 mAh g^{-1} after 50 cycles at 1 C. The $Li_{1.2}Mn_{0.54}Ni_{0.13}Co_{0.13}O_2$ coated with 3 wt% $LaNiO_3$ shows improvements in the discharge capacity with the initial value of 160.7 mAh g^{-1}, reaching the maximum of 207.6 mAh g^{-1} in the 14th cycle and retaining 190.3 mAh g^{-1} after 50 cycles at 1 C. Meanwhile, the 50 cycles capacity retention (92%) of 3 wt% $LaNiO_3$-coated sample is higher than 1 wt% and 5 wt% coating, which is equal to the pristine value.

In the first several cycles when the discharge capacity increases, it is responsible for low initial activation and high constant current density. Li_2MnO_3 phase is unstable due to the elimination oxygen vacancies and Li sites during charging inside the layered structure. The layer structure, rebuild by the lithium repeated intercalation/de-intercalation, gradually becomes stable after the first several activation cycles. Furthermore, the transformation is irretrievable, which brings large initial capacity loss. Therefore, the Li ions absolutely cannot enter into the layered structure by Li ions intercalation mechanism during the first discharging at high current density of 1 C. The discharge capacity of all samples decreases gradually after reaching the maximum, which indicates that the layer structure was completely activated after the first several cycles.

It is worth noting that, as introduced above, the initial capacity and Coulomb efficiency are improved, which implies that the initial activation was more or less promoted by the coating route. This may be attributed to the $LaNiO_3$ coating increasing the Li ions conduction and reducing the interface resistance. However, the discharge capacity of all samples reached the maximum after about 10 cycles at high current density of 1 C. It is considered that they have the same internal structures and phase composition.

Overall, the $LaNiO_3$ layer should be responsible for the enhanced high-rate electrochemical performance, which efficiently protects the cathode material from reacting with electrolyte as well as

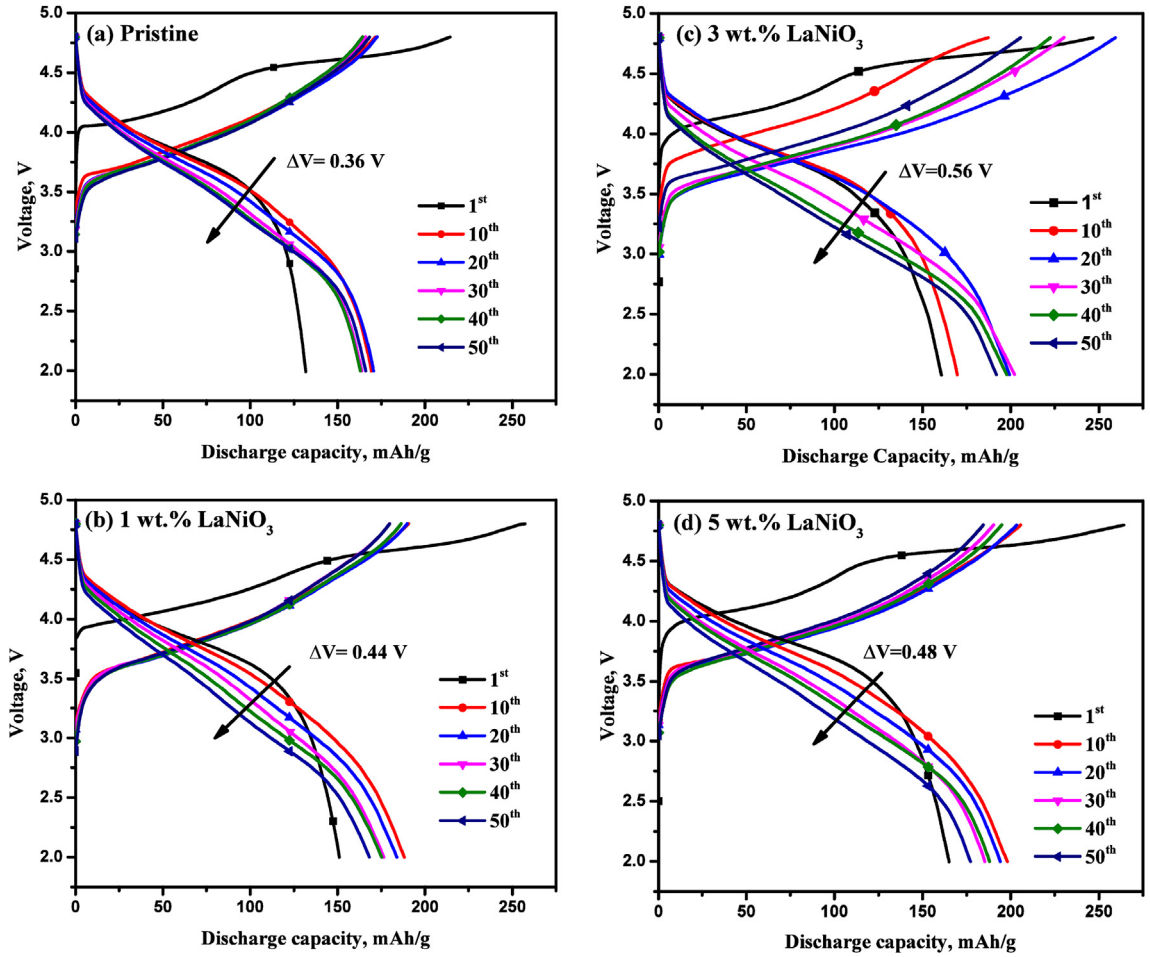

Fig. 7. Charge/discharge profiles of LMNC and $LaNiO_3$-coated LMNC electrodes during 50 cycles at 1 C between 2 and 4.8 V: (a) pristine, (b) 1 wt% $LaNiO_3$, (c) 3 wt% $LaNiO_3$, (d) 5 wt% $LaNiO_3$.

depressing the elimination rate of oxygen vacancies and Li sites during electrochemical cycling [27,37,38,43,45].

As seen from Fig. 6, the curve fluctuates with small amplitude, and the fluctuation amplitude tends to rise slightly as the content of $LaNiO_3$ increases. This phenomenon of curve fluctuation is routinely seen in similar literature reports [27,38,42,43]. As for the fluctuation, it could possibly be related to the inadequate lithium intercalation/de-intercalation process. The excessive $LaNiO_3$ may be responsible for the increased amplitudes for coating with 5 wt% $LaNiO_3$. In addition, an excessive dose of $LaNiO_3$ results in the capacity reduction, which may be attributed to two reasons. One reason may be because extra $LaNiO_3$ absorbed a lot of lithium ions to form $Li_{3x}La_{(2/3)-x}\square_{(1/3)-2x}NiO_3$, which cannot participate in the repeated intercalation/de-intercalation. On the other hand, it is presumably caused by the cation mixing on their surface and the formed solid electrolyte interphase film insulating layer.

The charge/discharge profiles of LMNC and $LaNiO_3$-coated LMNC electrodes in 1st, 10th, 20th, 30th, 40th and 50th cycles at 1 C are shown in Fig. 7. Except for the 1st cycle, the charge plateaus increase with the cycle number, while the discharge capacity fades gradually for all electrodes. This result indicates that the polarization of electrodes increases with the number of cycles [27]. The charge/discharge profiles of LMNC and $LaNiO_3$-coated LMNC electrodes agree well with the cyclic performance described above. The discharge midpoint voltage of the pristine electrode decays by 0.36 V (ΔV) from the 1st to 50th cycle, as indicated by the arrow in Fig. 7(a). One can also see from Fig. 7(b, c, d) that the ΔV values of $LaNiO_3$-coated LMNC electrodes are 0.44 V, 0.56 V, 0.48 V, corresponding to $LaNiO_3$ content of 1 wt%, 3 wt%, 5 wt%, respectively. Despite the $LaNiO_3$ coatings improving the charge/discharge capacity, the increasing ΔV values reflect that the $LaNiO_3$-coated LMNC electrodes show higher polarization at high rate of 1 C, compared with the pristine electrode.

Increasing electrode voltage decay ΔV may be attributed to the cation mixing (Ni) on their surface. This behavior can be explained as follows. The Ni ions in $LaNiO_3$ coating more or less participate in the redox reaction. Furthermore, in the charge/discharge cycles with high current density, Li ions repeatedly pass through the coating layer. The two behaviors are possible to affect the structure and Li ions conduction, which bring higher polarization and voltage decay. The small fluctuations of discharge (Fig. 6) also confirm the change of Li ions conduction.

Fig. 8 shows cyclic voltammetric profiles of (a) LMNC and (b) 3 wt% $LaNiO_3$-coated LMNC electrodes in the 1st and 2nd cycles between 2 V and 4.8 V at a scan rate of 0.1 mV/s. The cyclic voltammetric profiles reflect the oxidation-reduction reaction with cycles. As seen from Fig. 8, there are two high oxidation peaks in the 1st cycle, corresponding to the two charge plateaus at approximately 4 V and 4.5 V in Fig. 5. The oxidation peak at 4 V is relative to the oxidation of Ni^{2+} to Ni^{4+} and Co^{3+} to Co^{4+}. The second oxidation peak at 4.5 V can be ascribed to the irreversible electrochemical activation reaction (2), in which the Li_2MnO_3 phase is converted to Li_2O and MnO_2. Comparing the 1st and 2nd cycles, the second oxidation peak at 4.5 V in the 1st cycle disappears in the 2nd cycle. This phenomenon can explain the large irreversible capacity in the initial cycle. This is mainly because of the elimination of the oxide ion vacancies and the lithium ion sites.

The Nyquist plots recorded by the electrochemical impedance spectroscopy (EIS) of the pristine and 3 wt% $LaNiO_3$-coated LMNC electrodes are shown in Fig. 9(a) and (b). The equivalent circuit is given in Fig. 9(c). The EIS experiments were carried out at 4.3 V in the first and 50th cycles. As seen from the figures, all curves show two semicircles and a short slope line. According to multiple reports, the cell impedance is mainly due to the two semicircles, which reflect the resistance of Li ions migration through the surface

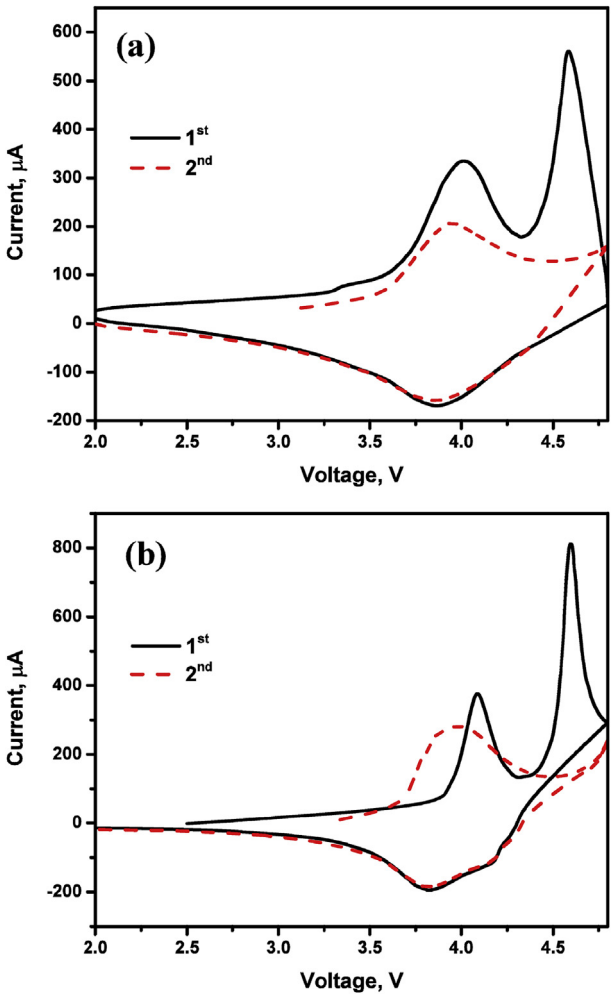

Fig. 8. Cyclic voltammetric profiles of: (a) LMNC and (b) 3 wt% $LaNiO_3$-coated LMNC electrode during the 1st and 2nd cycles between 2 and 4.8 V at 0.1 mV/s scan rate.

films (R_f) and the charge transfer resistance (R_{ct}) in the electrode/electrolyte interface [27,38,42,43], respectively. In general, R_s represents the solution resistance, CPE refers to the non-ideal double-layer capacitance, and W_o reflects the Warburg impedance. The values of R_f and R_{ct} were calculated and listed in Table 4. In the 1st cycle, the film resistance and charge transfer resistance of samples both decrease after coating with $LaNiO_3$. This demonstrates that 3 wt% $LaNiO_3$-coated electrodes can depress the side reaction in the electrode/electrolyte interface increasing the Li ion conduction. After 50 cycles, the R_{ct} value of 3 wt% $LaNiO_3$-coated LMNC shows much less increase than the pristine ones. In addition, the decrease in the R_f value of the pristine electrodes during 50 cycles may be attributed to the unstable SEI film, which is easy to be destroyed. However, the R_f value of coated samples presents a little change, evidently indicating that the $LaNiO_3$ is helpful to stabilize the film. Overall, the electrochemical performance of the LMNC electrodes can be enhanced by coating with $LaNiO_3$.

4. Conclusions

$LaNiO_3$-coated LMNC cathodes were fabricated via co-precipitation method and surface coated $LaNiO_3$ via a sol-gel process. A thin $LaNiO_3$ layer is evenly coated on the surface of LMNC particles. There is no effect on the crystal structure of the materials

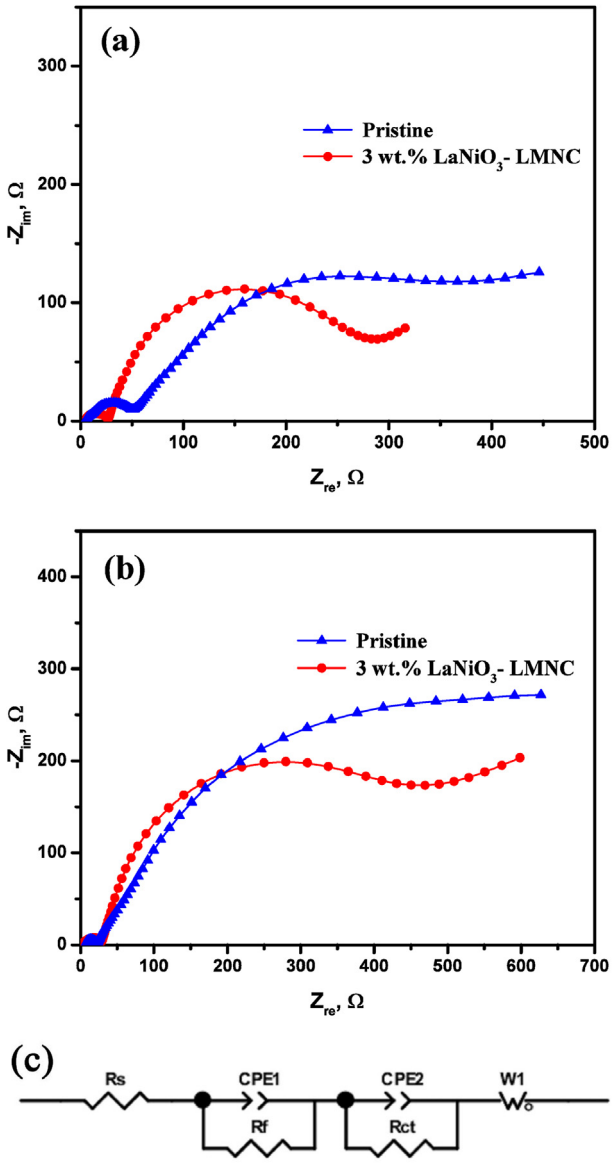

Fig. 9. The Nyquist plots of pristine and 3 wt% $LaNiO_3$-coated LMNC electrodes: (a) the initial cycle, (b) the 50th cycle, (c) the equivalent circuit.

Table 4
The film resistance R_f and charge transfer resistance R_{ct} of the pristine and $LaNiO_3$-coated samples in the 1st and 50th cycles.

Samples	Pristine		3 wt% $LaNiO_3$-coated LMNC	
Cycle	R_f (Ω)	R_{ct} (Ω)	R_f (Ω)	R_{ct} (Ω)
1st	48.45	467.1	24.14	242.2
50th	15.84	980.4	25.96	583.0

after modification with $LaNiO_3$. The surface modification of $LaNiO_3$ leads to a great enhancement in the specific capacity cycling stability and rate capacity of the Li-rich cathode. The optimal $LaNiO_3$-coating content is 3 wt%, which presents improved initial charge/discharge capacity of 405.4/285.1 mAh g^{-1} and 264.1/165.1 mAh g^{-1} at 0.1 C rate and 1 C. The initial Coulombic efficiency reached the maximum of 70% and 65% at 0.1 C and 1 C, respectively. As seen from the cycling performance profiles at 1 C rate, the 3 wt% $LaNiO_3$-coated $Li_{1.2}Mn_{0.54}Ni_{0.13}Co_{0.13}O_2$ samples exhibit highest discharge capacity compared to pristine and other content of $LaNiO_3$ during 50 cycles. The film resistance and charge transfer resistance both decrease after coating with $LaNiO_3$. This study shows that $LaNiO_3$ is an efficient modifier to enhance the electrochemical performance of Li-rich cathode materials. The stable and thin $LaNiO_3$ conducting coating layer had not only protected the electrode structure from destruction, but also provided an effective barrier to prevent the side reaction of electrolyte and electrode without damage to ions conductivity and diffusion during cycling. The $LaNiO_3$-coated $Li_{1.2}Mn_{0.54}Ni_{0.13}Co_{0.13}O_2$ cathode could be a promising candidate for new generation of high rate rechargeable lithium-ion batteries.

References

[1] B. Huang, P. Shi, Z. Liang, M. Chen, Y. Guan, Effects of sintering on the performance of hydrogen storage alloy electrode for high-power Ni/MH batteries, J. Alloys Compd. 394 (2005) 303–307.
[2] J.M. Chen, C.H. Hsu, Y.R. Lin, M.H. Hsiao, T.K. Fey, High-power $LiFePO_4$ cathode materials with a continuous nano carbon network for lithium-ion batteries, J. Power Sources 184 (2008) 498–502.
[3] K.S. Tan, M.V. Reddy, G.V.S. Rao, B.V.R. Chowdari, High-performance $LiCoO_2$ by molten salt ($LiNO_3$: LiCl) synthesis for Li-ion batteries, J. Power Sources 147 (2005) 241–248.
[4] M.V. Reddy, A. Sakunthala, S. Selvashekarapandian, B.V.R. Chowdari, Preparation, comparative energy storage properties, and impedance spectroscopy studies of environmentally friendly cathode, $Li(MMn_{11/6})O_4$ (M=$Mn_{1/6}$,$Co_{1/6}$,($Co_{1/12}$ $Cr_{1/12}$)), J. Phys. Chem. C 117 (2013) 9056–9064.
[5] T.K. Fey, K.P. Huang, H.M. Kao, W.H. Li, A polyethylene glycol-assisted carbothermal reduction method to synthesize $LiFePO_4$ using industrial raw materials, J. Power Sources 196 (2011) 2810–2818.
[6] Z.H. Lu, D.D. Macneil, J.R. Dahn, Layered cathode materials $Li[Ni_xLi_{(1/3-2x/3)}Mn_{(2/3-x/3)}]O_2$ for lithium-ion batteries, Electrochem. Electrochem. Solid State Lett. 7 (2001) A503–A506.
[7] Z. Lu, J.R. Dahn, Understanding the anomalous capacity of $Li/Li[Ni_xLi_{(1/3-2x/3)}Mn_{(2/3-x/3)}]O_2$ cells using in situ x-ray diffraction and electrochemical studies, J. Electrochem. Soc. 149 (2002) A815–A822.
[8] X.J. Guo, Y.X. Li, M. Zheng, J.M. Zheng, J. Li, Z.L. Gong, Y. Yang, Structural and electrochemical characterization of $xLi[Li_{1/3}Mn_{2/3}]O_2\cdot(1-x)Li[Ni_{1/3}Mn_{1/3}Co_{1/3}]O_2$ ($0\leq x\leq 0.9$) as cathode materials for lithium ion batteries, J. Power Sources 184 (2008) 414–419.
[9] C.V. Rao, J. Soler, R. Katiyar, J. Shojan, W.C. West, R.S. Katiyar, Investigations on electrochemical behavior and structural stability of $Li_{1.2}Mn_{0.54}Ni_{0.13}Co_{0.13}O_2$ lithium-ion cathodes via in-situ and ex-situ Raman spectroscopy, J. Phys. Chem. C 118 (2014) 14133–14141.
[10] C.S. Johnson, J.S. Kim, C. Lefief, N. Li, J.T. Vaughey, M.M. Thackeray, The significance of the Li_2MnO_3 component in composite $xLi_2MnO_3\cdot(1-x)LiMn_{0.5-x}Ni_{0.5}O_2$ electrodes, Electrochem. Commun. 6 (2004) 1085–1091.
[11] M.M. Thackeray, S.H. Kang, C.S. Johnson, J.T. Vaughey, R. Benedek, S.A. Hackney, Li_2MnO_3-stabilized $LiMO_2$ (M = Mn, Ni, Co) electrodes for lithium-ion batteries, J. Mater. Chem. 17 (2007) 3112–3125.
[12] H. Yu, Y. Wang, D. Asakura, E. Hosono, T. Zhang, H. Zhou, Electrochemical kinetics of the $0.5Li_2MnO_30.5LiMn_{0.42}Ni_{0.42}Co_{0.16}O_2$ 'composite' layered cathode material for lithium-ion batteries, RSC Adv. 2 (2012) 8797–8807.
[13] H.Z. Zhang, Q.Q. Qiao, G.R. Li, S.H. Ye, X.P. Gao, Surface nitridation of Li-rich layered $Li(Li_{0.17}Ni_{0.25}Mn_{0.58})O_2$ oxide as cathode material for lithium-ion battery, J. Mater. Chem. 22 (2012) 13104–13109.
[14] S.H. Kang, P. Kempgens, S. Greenbaum, A.J. Kropf, K. Amine, M.M. Thackeray, Interpreting the structural and electrochemical complexity of $0.5Li_2MnO_3\cdot0.5LiMO_2$ electrodes for lithium batteries (M = $Mn_{0.5-x}Ni_{0.5-x}Co_{2x}$, $0\leq x\leq 0.5$), J. Mater. Chem. 17 (2007) 2069–2077.
[15] A.R. Armstrong, M. Holzapfel, P. Novák, C.S. Johnson, S.H. Kang, M.M. Thackeray, P.G. Bruce, Demonstrating oxygen loss and associated structural reorganization in the lithium battery cathode $Li[Ni_{0.2}Li_{0.2}Mn_{0.6}]O_2$, J. Am. Chem. Soc. 128 (2006) 8694.
[16] F. Fu, Y.P. Deng, C.H. Shen, G.L. Xu, X.X. Peng, Q. Wang, Y.F. Xu, J.C. Fang, L. Huang, S.G. Sun, A hierarchical micro/nanostructured $0.5Li_2MnO_3\cdot0.5LiMn_{0.4}Ni_{0.3}Co_{0.3}O_2$ material synthesized by solvothermal route as high rate cathode of lithium ion battery, Electrochem. Commun. 44 (2014) 54–58.
[17] D. Wang, I. Belharouak, L.H. Ortega, X. Zhang, R. Xu, D. Zhou, G. Zhou, K. Amine, Synthesis of high capacity cathodes for lithium-ion batteries by morphology-tailored hydroxide co-precipitation, J. Power Sources 274 (2015) 451–457.
[18] S.H. Kang, C.S. Johnson, J.T. Vaughey, K. Amine, M.M. Thackeray, The effects of acid treatment on the electrochemical properties of $0.5Li_2MnO_3\cdot0.5LiNi_{0.44}Co_{0.25}Mn_{0.31}O_2$ electrodes in lithium cells 153 (2006).
[19] S.H. Kang, M.M. Thackeray, Stabilization of $xLi_2MnO_3\cdot(1-x)LiMO_2$ electrode surfaces (M=Mn, Ni, Co) with mildly acidic, fluorinated solutions, J. Electrochem. Soc. 155 (2008).
[20] W. He, D. Yuan, J. Qian, X. Ai, H. Yang, Y. Cao, Enhanced high-rate capability

and cycling stability of Na-stabilized layered $Li_{1.2}[Co_{0.13}Ni_{0.13}Mn_{0.54}]O_2$ cathode material, J. Mater. Chem. A 1 (2013) 11397–11403.
[21] B. Song, M.O. Lai, L. Lu, Influence of Ru substitution on Li-rich $0.55Li_2MnO_3 \cdot 0.45LiNi_{1/3}Co_{1/3}Mn_{1/3}O_2$ cathode for Li-ion batteries, Electrochim. Acta 80 (2012) 187–195.
[22] X. Jin, Q. Xu, H. Liu, X. Yuan, Y. Xia, Excellent rate capability of Mg doped $Li[Li_{0.2}Ni_{0.13}Co_{0.13}Mn_{0.54}]O_2$ cathode material for lithium-ion battery, Electrochim. Acta 136 (2014) 19–26.
[23] Q. Li, G. Li, C. Fu, D. Luo, J. Fan, L. Li, K^+-doped $Li_{1.2}Mn_{0.54}Co_{0.13}Ni_{0.13}O_2$: a novel cathode material with an enhanced cycling stability for lithium-ion batteries, ACS Appl. Mater. Interfaces 6 (2014) 10330.
[24] A.S. Ulihin, A.B. Slobodyuk, N.F. Uvarov, O.A. Kharlamova, V.P. Isupov, V.Y. Kavun, Conductivity and NMR study of composite solid electrolytes based on lithium perchlorate, Solid State Ionics 179 (2008) 1740–1744.
[25] Y. Wu, A.V. Murugan, A. Manthiram, Surface modification of high capacity layered $Li[Li_{0.2}Mn_{0.54}Ni_{0.13}Co_{0.13}]O_2$ cathodes by $AlPO_4$, J. Electrochem. Soc. 155 (2008) A635–A641.
[26] J.H. Ju, S.W. Cho, S.G. Hwang, S.R. Yun, Y. Lee, M.J. Han, M.J. Hwang, K.M. Kim, K.S. Ryu, Electrochemical performance of $Li[Co_{0.1}Ni_{0.15}Li_{0.2}Mn_{0.55}]O_2$ modified by carbons as cathode materials, Electrochim. Acta 56 (2011) 8791–8796.
[27] C. Lu, H. Wu, Y. Zhang, H. Liu, B. Chen, N. Wu, S. Wang, Cerium fluoride coated layered oxide $Li_{1.2}Mn_{0.54}Ni_{0.13}Co_{0.13}O_2$ as cathode materials with improved electrochemical performance for lithium ion batteries, J. Power Sources 267 (2014) 682–691.
[28] W. Yuan, H.Z. Zhang, Q. Liu, G.R. Li, X.P. Gao, Surface modification of $Li(Li_{0.17}Ni_{0.2}Co_{0.05}Mn_{0.58})O_2$ with CeO_2 as cathode material for Li-ion batteries, Electrochim. Acta 135 (2014) 199–207.
[29] X. Bian, Q. Fu, X. Bie, P. Yang, H. Qiu, Q. Pang, G. Chen, F. Du, Y. Wei, Improved electrochemical performance and thermal stability of Li-excess $Li_{1.18}Co_{0.15}Ni_{0.15}Mn_{0.52}O_2$ cathode material by Li_3PO_4 surface coating, Electrochim. Acta 174 (2015) 875–884.
[30] P. Knauth, Inorganic solid Li ion conductors: an overview, Solid State Ionics 180 (2009) 911–916.
[31] R. Schmidberger, W. Donitz, Mixed Oxides for the Electrodes of Electrochemical High Temperature Cells with Solid Electrolyte, and Process for Their Manufacture, 1980.
[32] A.V. Joshi, J.J. Steppan, D.M. Taylor, S. Elangovan, Solid electrolyte materials, devices, and applications, Cheminform 13 (2004) 619–625.
[33] D.O. Bannikov, V.A. Cherepanov, Thermodynamic properties of complex oxides in the La–Ni–O system, J. Solid State Chem. 179 (2006) 2721–2727.
[34] S. Miyake, S. Fujihara, T. Kimura, Characteristics of oriented $LaNiO_3$ thin films fabricated by the sol–gel method, J. Eur. Ceram. Soc. 21 (2001) 1525–1528.
[35] J. Jia, G. Zhao, L. Lei, X. Wang, Preparation of $LaNiO_3/SrTiO_3/LaNiO_3$ capacitor structure through sol-gel process, Ceram. Int. 42 (2016) 9762–9768.
[36] K.A. Jarvis, Z. Deng, L.F. Allard, A. Manthiram, P.J. Ferreira, Atomic structure of a lithium-rich layered oxide material for lithium-ion batteries: evidence of a solid solution, Chem. Mater. 23 (16) (2011) 3614–3621.
[37] K. Jarvis, Z. Deng, A. Manthiram, P.J.F.L. Allard, Understanding structural defects in lithium-rich layered oxide cathodes by aberration-corrected STEM, J. Mater. Chem. 22 (2012) 11550–11555.
[38] Z. Wang, E. Liu, C. He, C. Shi, J. Li, N. Zhao, Effect of amorphous $FePO_4$ coating on structure and electrochemical performance of $Li_{1.2}Ni_{0.13}Co_{0.13}Mn_{0.54}O_2$ as cathode material for Li-ion batteries, J. Power Sources 236 (2013) 25–32.
[39] J. Wang, B. Qiu, H. Cao, Y. Xia, Z. Liu, Electrochemical properties of $0.6Li[Li_{1/3}Mn_{2/3}]O_2$ - $0.4LiNi_xMnyCo_{1-x-y}O_2$ cathode materials for lithium-ion batteries, J. Power Sources 218 (2012) 128–133.
[40] Z.H. Lu, L.Y. Beaulieu, R.A. Donaberger, C.L. Thomas, J.R. Dahn, Synthesis, structure, and electrochemical behavior of $Li\ Ni_xLi_{1/3-2x/3}Mn_{2/3-x/3}\ O_2$, J. Electrochem. Soc. 149 (2002) A778–A791.
[41] X. Luo, X. Wang, L. Liao, X. Wang, S. Gamboa, P.J. Sebastian, Effects of synthesis conditions on the structural and electrochemical properties of layered $Li[Ni_{1/3}Co_{1/3}Mn_{1/3}]O_2$ cathode material via the hydroxide co-precipitation method LIB SCITECH, J. Power Sources 161 (2006) 601–605.
[42] D. Mohanty, S. Kalnaus, R.A. Meisner, K.J. Rhodes, J. Li, E.A. Payzant, D.L. Wood, C. Daniel, Structural transformation of a lithium-rich $Li_{1.2}Co_{0.1}Mn_{0.55}Ni_{0.15}O_2$ cathode during high voltage cycling resolved by in situ X-ray diffraction, J. Power Sources 229 (2013) 239–248.
[43] L. Zhou, M. Tian, Y. Deng, Q. Zheng, C. Xu, D. Lin, La_2O_3-coated $Li_{1.2}Mn_{0.54}Ni_{0.13}Co_{0.13}O_2$ as cathode materials with enhanced specific capacity and cycling stability for lithium-ion batteries, Ceram. Int. 42 (2016) 15623–15633.
[44] S.J. Shi, J.P. Tu, Y.J. Mai, Y.Q. Zhang, C.D. Gu, X.L. Wang, Effect of carbon coating on electrochemical performance of $Li_{1.048}Mn_{0.381}Ni_{0.286}Co_{0.286}O_2$ cathode material for lithium-ion batteries, Electrochim. Acta 63 (2012) 112–117.
[45] W. He, J. Qian, Y. Cao, X. Ai, H. Yang, Improved electrochemical performances of nanocrystalline $Li[Li_{0.2}Mn_{0.54}Ni_{0.13}Co_{0.13}]O_2$ cathode material for Li-ion batteries, RSC Adv. 2 (2012) 3423–3429.